

Layout of these lectures

- Introduction
- General remarks
- Model development and validation
- **The Earth energy budget**
- **Soil/Water contrasts**
- Snow hydrology
- Snow atmosphere coupling
- Vegetation cycle
- Carbon dioxide

Lecture 1

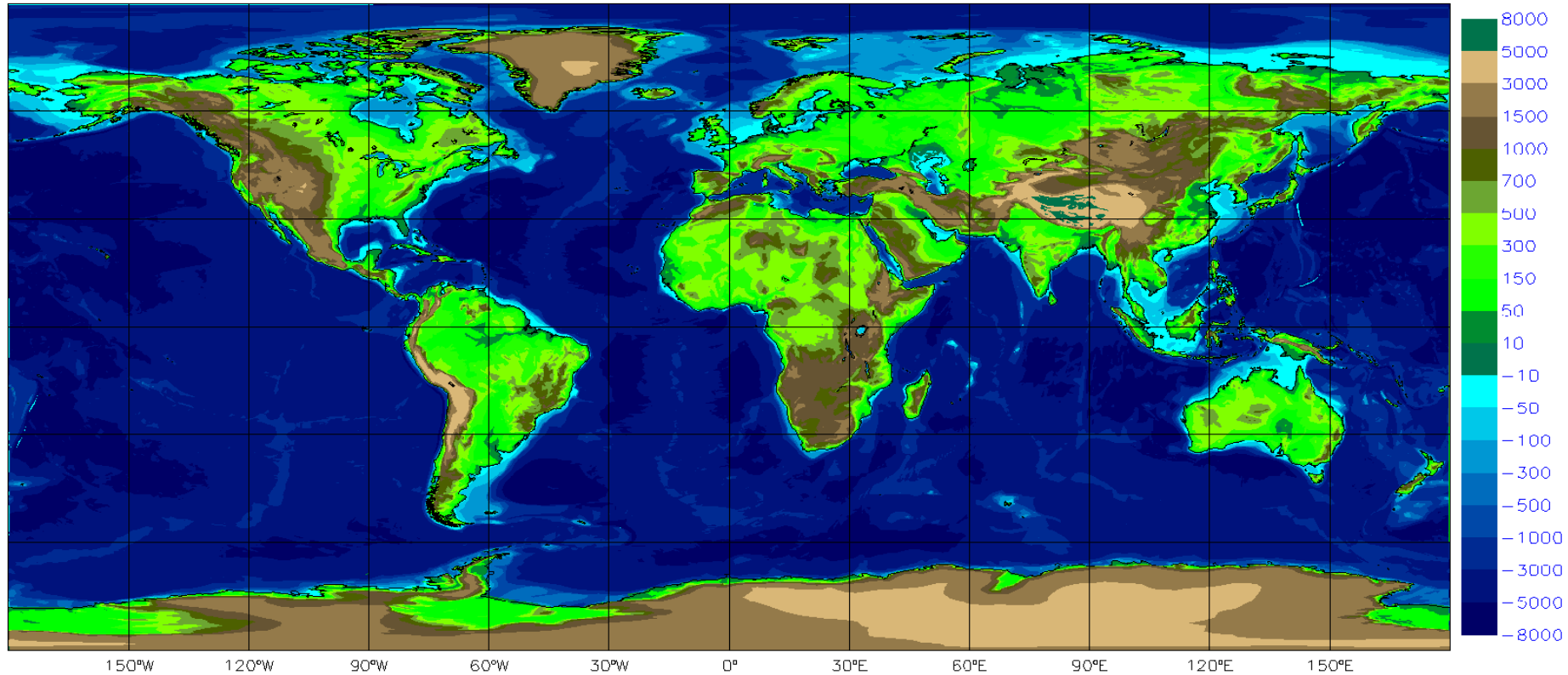
Lecture 2

Lecture 3

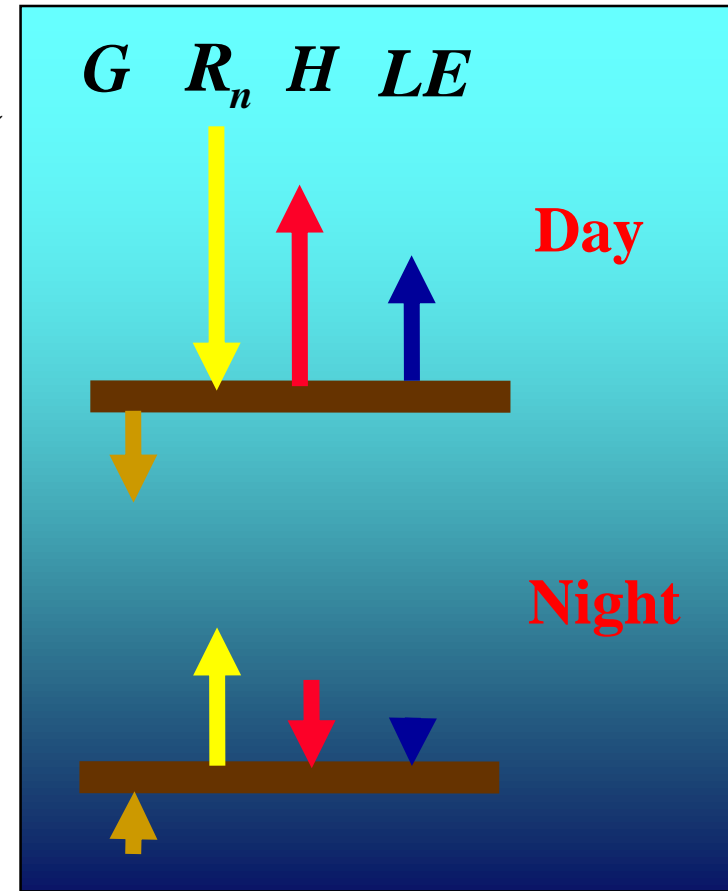
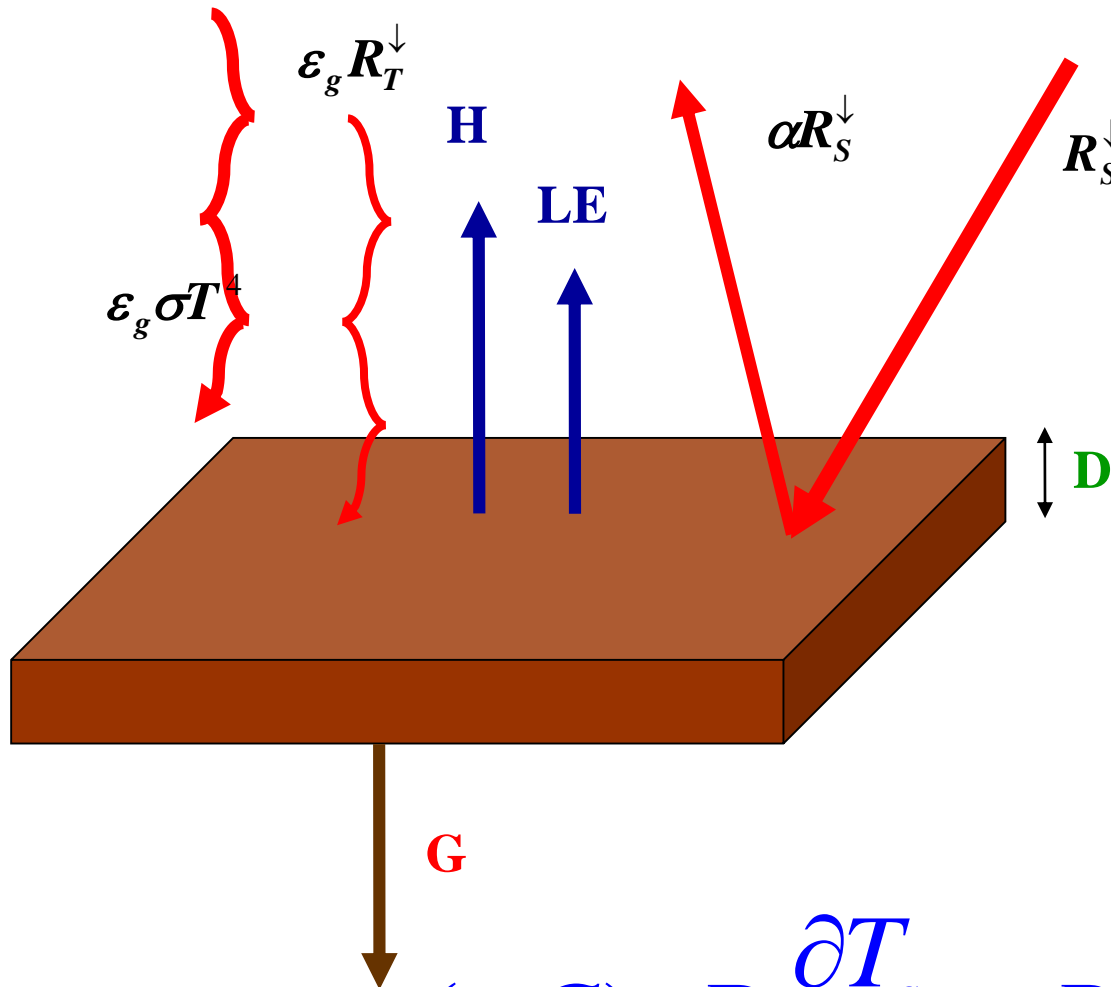
Lecture 4

The IFS Earth orography and bathymetry

land orography and ocean&lakes bathymetry (meters above/below sea-level, climate.v009, T1279)



Thermal budget of a ground layer at the surface



$$(\rho C)_g D \frac{\partial T_s}{\partial t} = R_n + H + LE + G$$

The surface radiation

Surface albedo

Surface emissivity

Skin temperature

- In some cases (snow, sea ice, dense canopies) the impinging solar radiations penetrates the “ground” layer and is absorbed at a variable depth. In those cases, an **extinction coefficient** is needed.

Table 3.1
Radiative Properties of Natural Surfaces^a

Surface type	Other specifications	Albedo (a)	Emissivity (ε)
Water	Small zenith angle	0.03–0.10	0.92–0.97
	Large zenith angle	0.10–0.50	0.92–0.97
Snow	Old	0.40–0.70	0.82–0.89
	Fresh	0.45–0.95	0.90–0.99
Ice	Sea	0.30–0.40	0.92–0.97
	Glacier	0.20–0.40	
Bare sand	Dry	0.35–0.45	0.84–0.90
	Wet	0.20–0.30	0.91–0.95
Bare soil	Dry clay	0.20–0.35	0.95
	Moist clay	0.10–0.20	0.97
	Wet fallow field	0.05–0.07	
Paved	Concrete	0.17–0.27	0.71–0.88
	Black gravel road	0.05–0.10	0.88–0.95
Grass	Long (1 m)	0.16–0.26	0.90–0.95
	Short (0.02 m)		
Agricultural	Wheat, rice, etc.	0.10–0.25	0.90–0.99
	Orchards	0.15–0.20	0.90–0.95
Forests	Deciduous	0.10–0.20	0.97–0.98
	Coniferous	0.05–0.15	0.97–0.99

^a Compiled from Sellers (1965), Kondratyev (1969), and Oke (1978).

Arya, 1988

The other terms

Sensible heat flux

$$H = \rho C_h u_L (C_p T_L + gz - C_p T_{sk})$$

$$C_h = f(Ri_B, z_{oh}, z_{om})$$

z_{oh}, z_{om} specify the surface

Evaporation

$$E = \rho C_h u_L [q_L - q_s] = \rho C_h u_L [a_L q_L - a_s q_{sat}(T_{sk}, p_s)]$$

$$a_{L,s} = f(q_L, T_s)$$

Ground heat flux

$$(\rho C)_g \frac{\partial T_s}{\partial t} = -\frac{\partial G}{\partial z} = \frac{\partial}{\partial z} \lambda_T \frac{\partial T}{\partial z}$$

$$(\rho C)_g, \lambda_T = f(\text{soil type, other soil characteristics})$$

HTESEL

- **Skin** layer at the interface between soil (snow) and atmosphere; **no thermal inertia**, instantaneous energy balance
- At the interface soil/atmosphere, each grid-box is divided into fractions (**tiles**), each fraction with a different functional behaviour. The different tiles see the **same atmospheric** column above and the **same soil** column below.

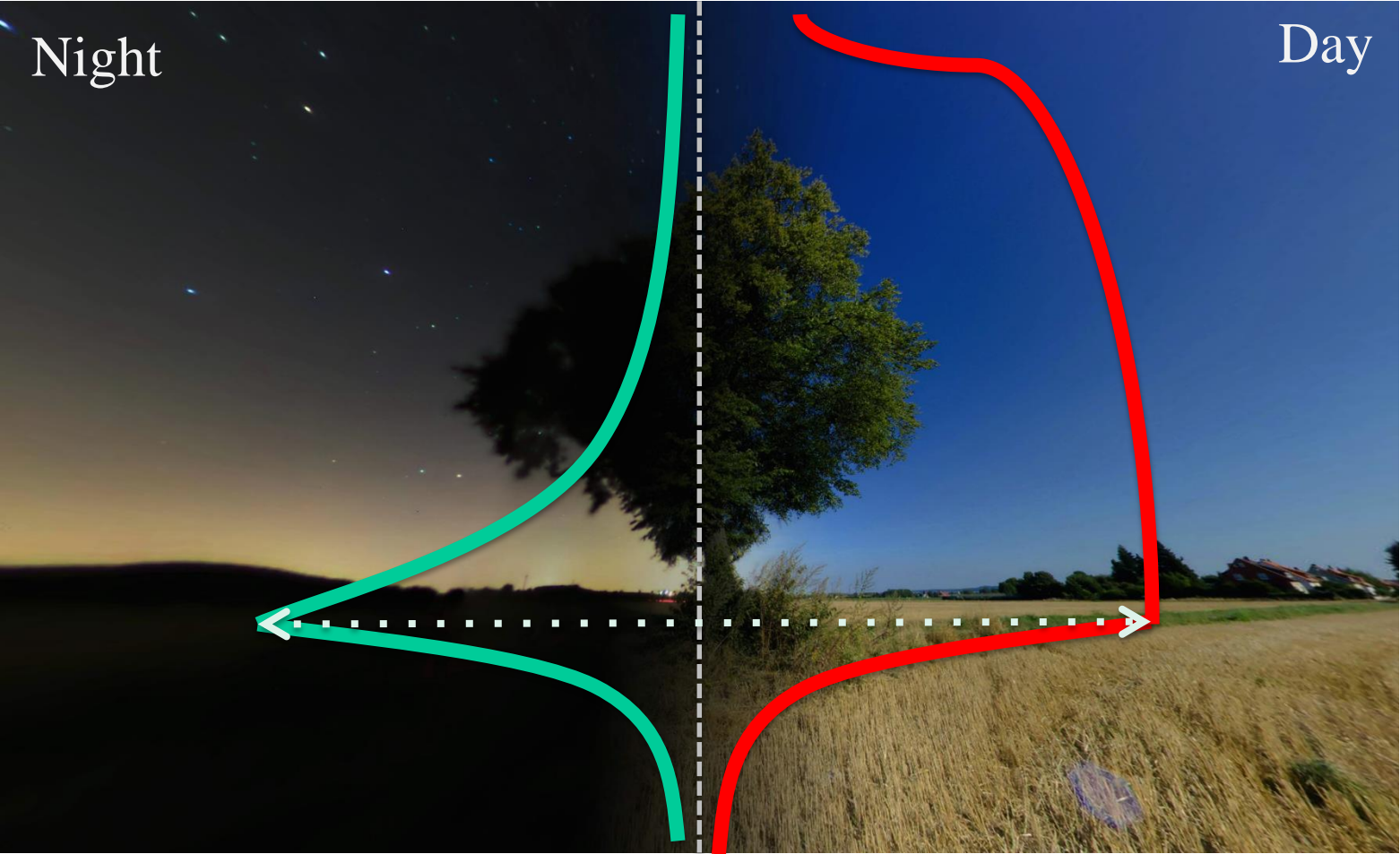
$$G_i = \Lambda_{sk,i} (T_s - T_{sk,i})$$

i index for tile

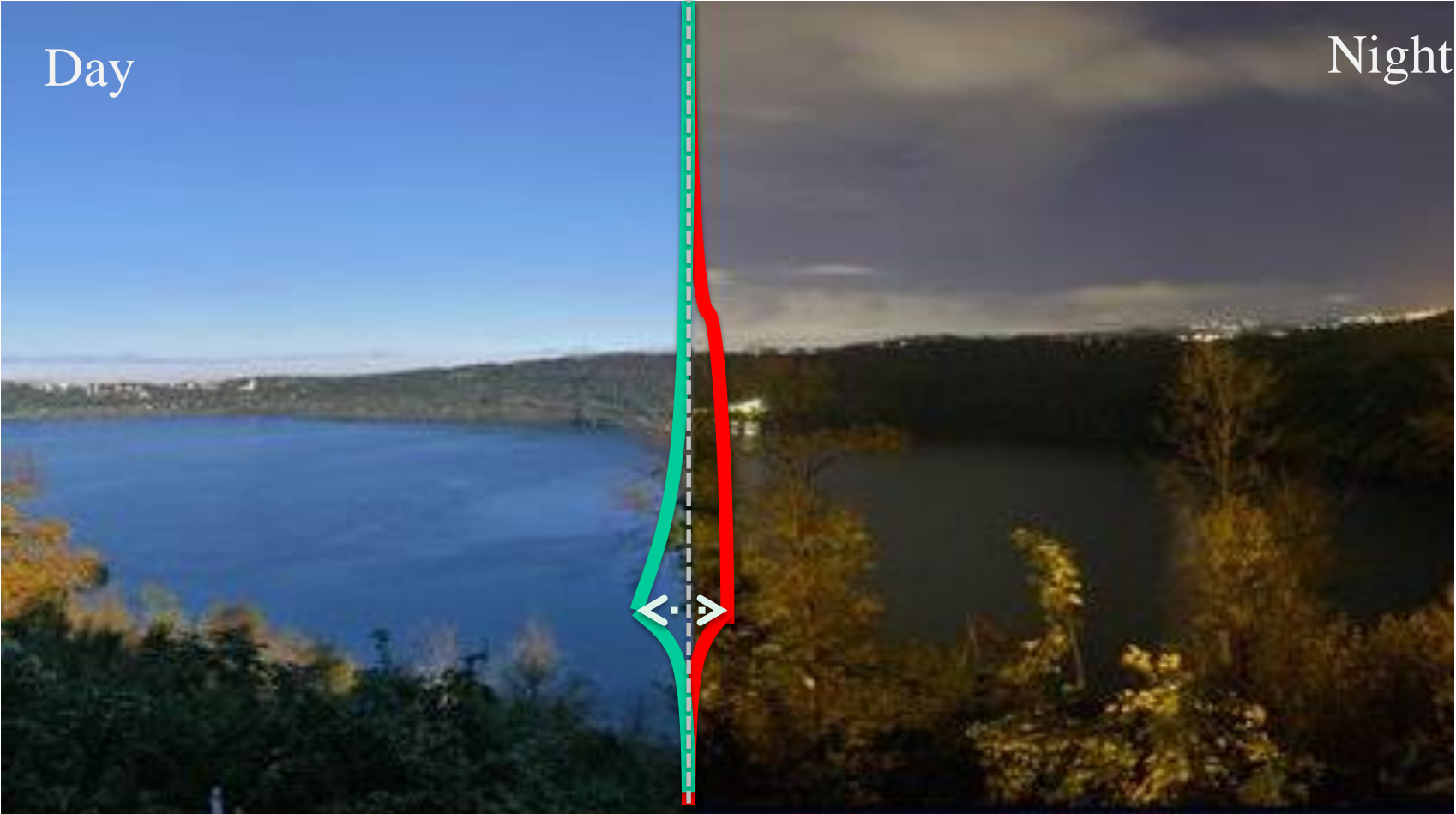
$$i = 1, \dots, N$$

- If there are N tiles, there will be N fluxes, N skin temperatures per grid-box
- There are currently up to 6 tiles over land ($N=6$)

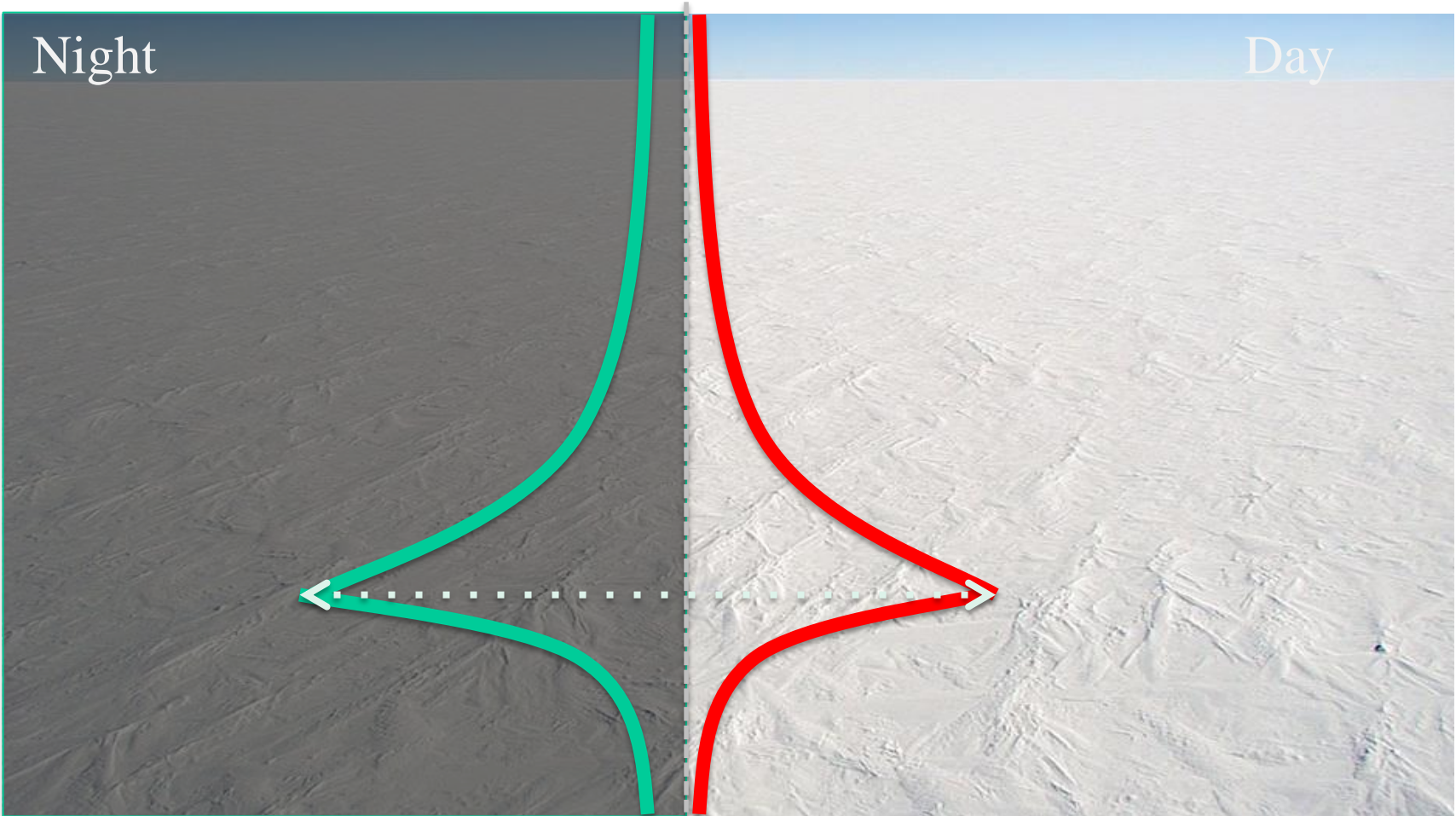
Coupling and diurnal cycle: vegetation



Coupling and diurnal cycle: lakes



Coupling and diurnal cycle: snow and ice



HTESEL skin temperature equation

$$(1 - \alpha_i)R_S^\downarrow + \varepsilon_g R_T^\downarrow - \varepsilon_g \sigma T_{sk,i}^4 + \\ \rho C_{h,i} u_L (C_p T_L + gz - C_p T_{sk,i}) + \\ \rho C_{h,i} u_L [a_{L,i} q_L - a_{s,i} q_{sat}(T_{sk,i}, p_s)] + \\ \Lambda_{sk,i} (T_s - T_{sk,i}) = 0$$

- **Grid-box quantities**

$$H = \sum_i C_i H_i$$

$$E = \sum_i C_i E_i$$

$$T_{sk} = \sum_i C_i T_{sk,i}$$

C_i Tile fraction

Ground heat flux

$$(\rho C)_g \frac{\partial T_s}{\partial t} = - \frac{\partial G}{\partial z} = \frac{\partial}{\partial z} \lambda_T \frac{\partial T}{\partial z}$$

$(\rho C)_g$ Soil volumetric heat capacity

λ_T Thermal conductivity

$k = \frac{\lambda_T}{(\rho C)_g}$ Thermal diffusivity

For an homogeneous soil,

$$\frac{\partial T_s}{\partial t} = k \frac{\partial^2 T}{\partial z^2}$$

•Top

•Bottom No heat flux

Diurnal cycle of soil temperature

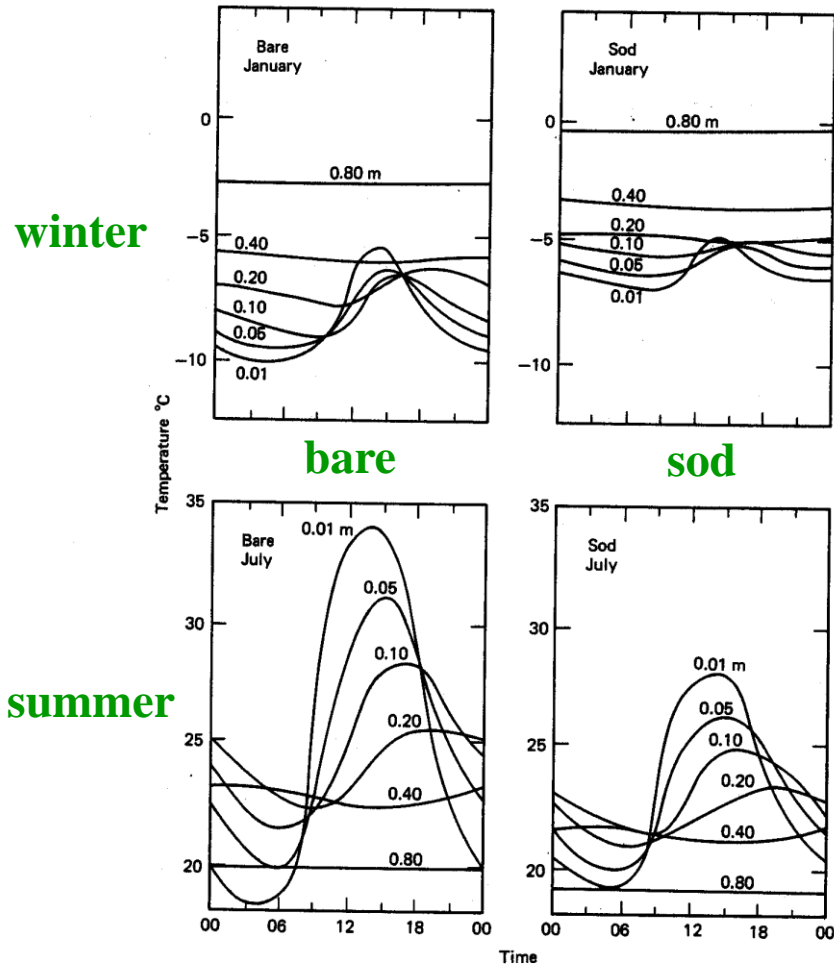


Fig. 2.2 Average hourly soil temperature under bare and sod-covered soil at St. Paul, Minnesota in January (top) and July (bottom). Soil depth is shown in m (after Baker, 1965).

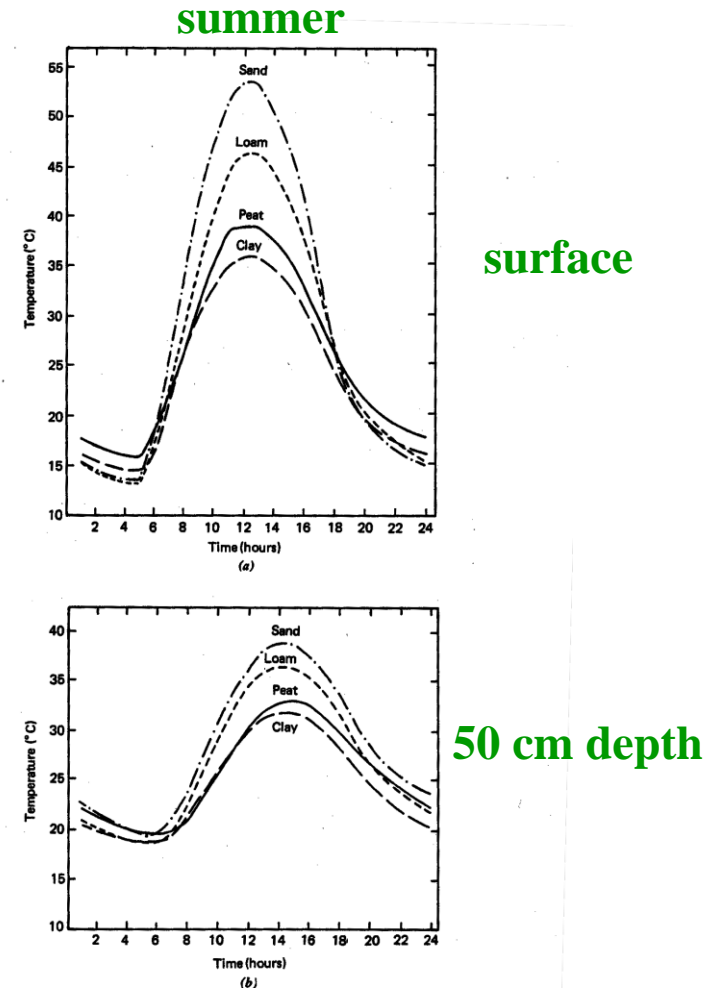
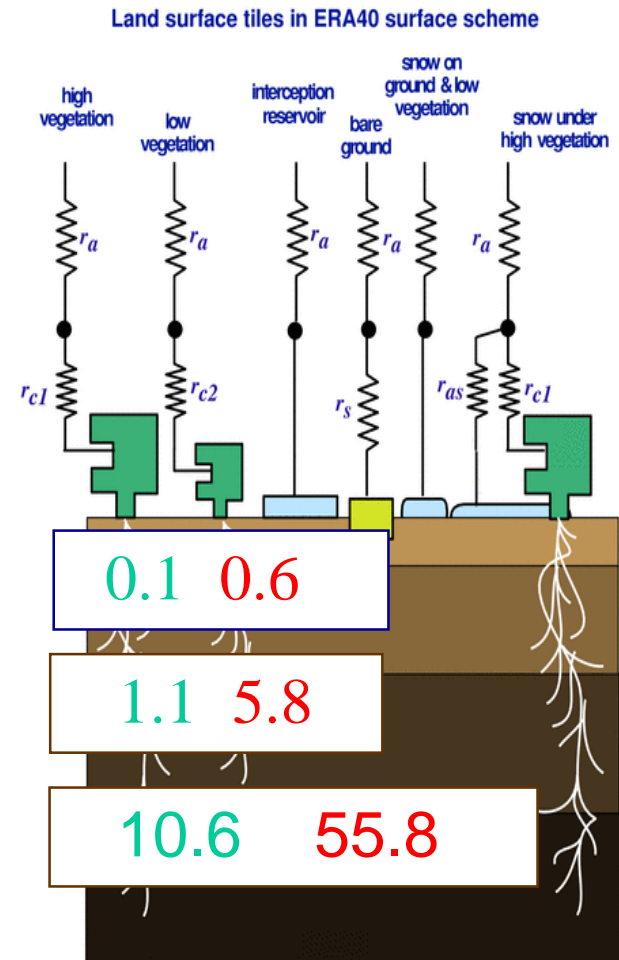


Fig. 2.6 Daily course of temperature (a) at the surface and (b) at a depth of 50 mm on clear summer days at Sapporo, Japan (after Yakuwa, 1946).

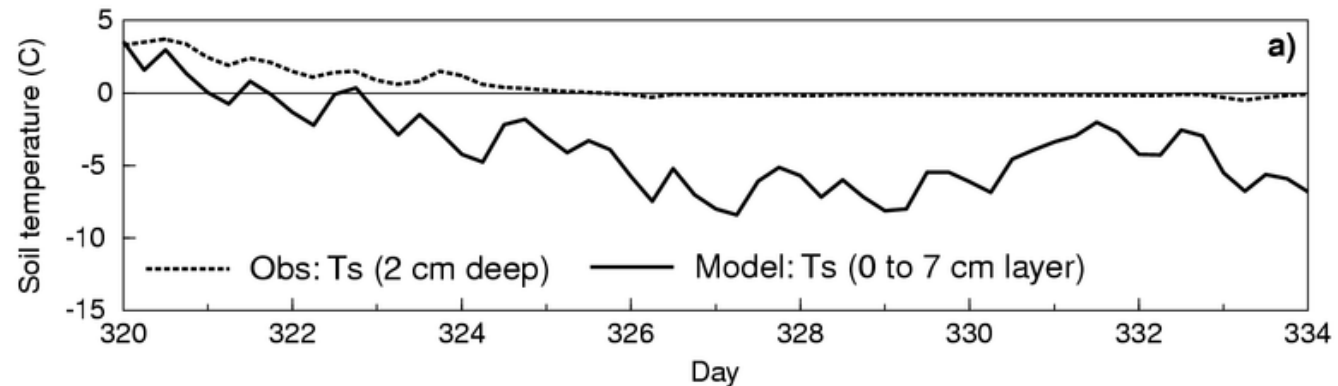
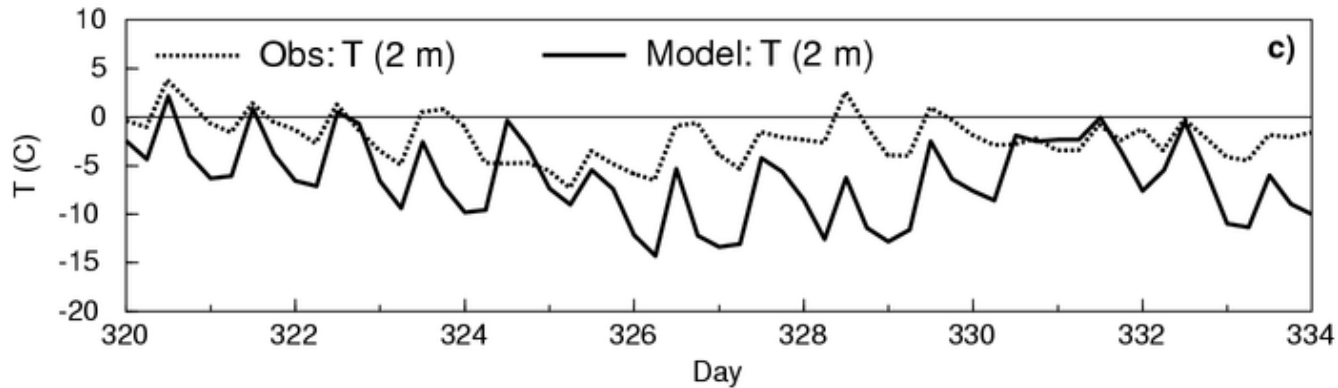
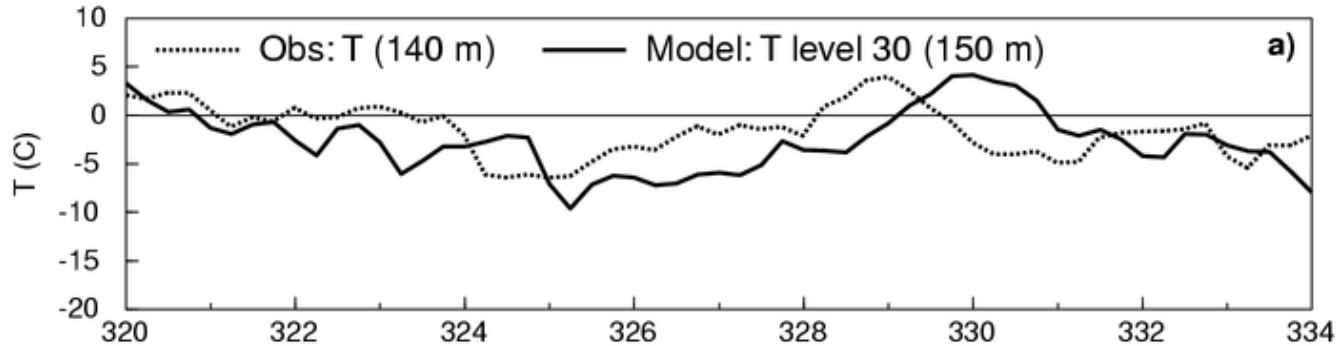
HTESSSEL heat transfer

- Solution of heat transfer equation with the soil discretized in **4 layers**, depths 7, 21, 72, and 189 cm.
- **No-flux bottom** boundary condition
- Heat conductivity dependent on soil water
- Thermal effects of **soil water phase change**



Case study: winter (1)

Model vs observations, Cabauw, The Netherlands, 2nd half of November 1994

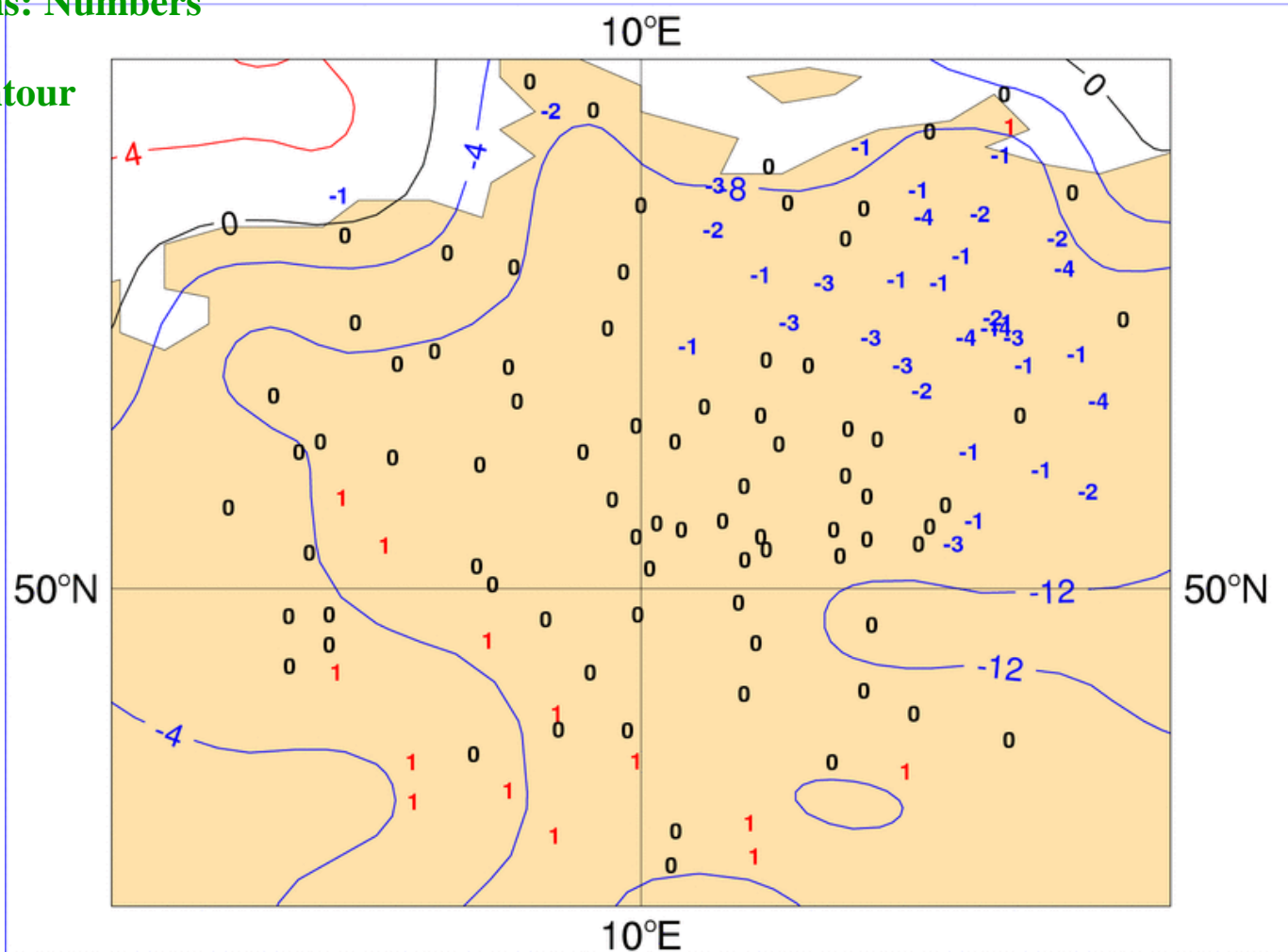


Case study: winter (2)

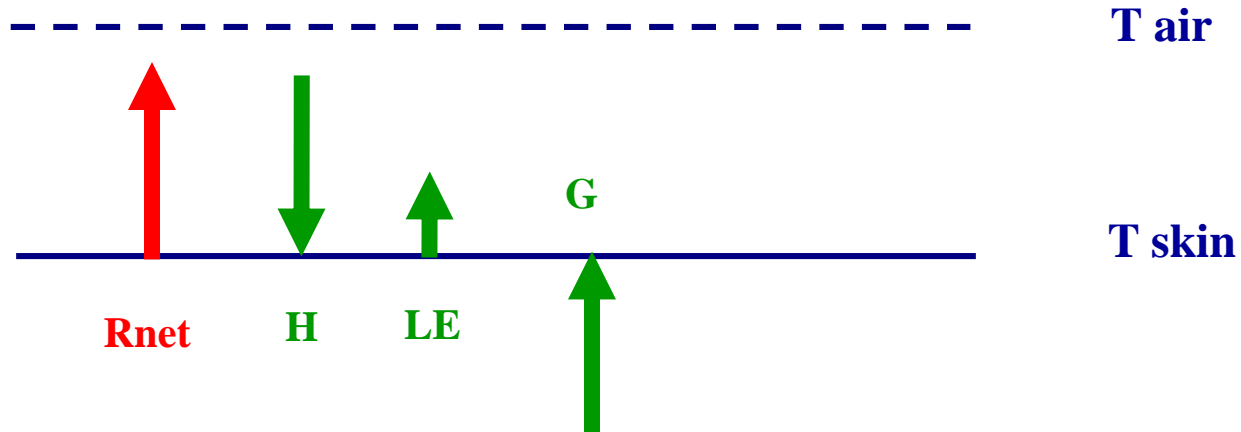
Soil Temperature, North Germany, Feb 1996: Model (28-100 cm) vs OBS 50 cm

Observations: Numbers

Model: Contour



Case study: winter (3)



$$H = \rho C_p |U_{air}| C_{Hn} f(Ri) (T_{air} - T_{sk})$$

● Model bias:

- Net radiation (R_{net}) too large
- Sensible heat (H) too small
 - But $(T_{air} - T_{sk})$ too large (too large diurnal cycle)
 - Therefore $f(Ri)$ problem
- Soil does not freeze (soil temperature drops too quickly seasonally)

Stability functions

Soil water freezing

Winter: Soil water freezing

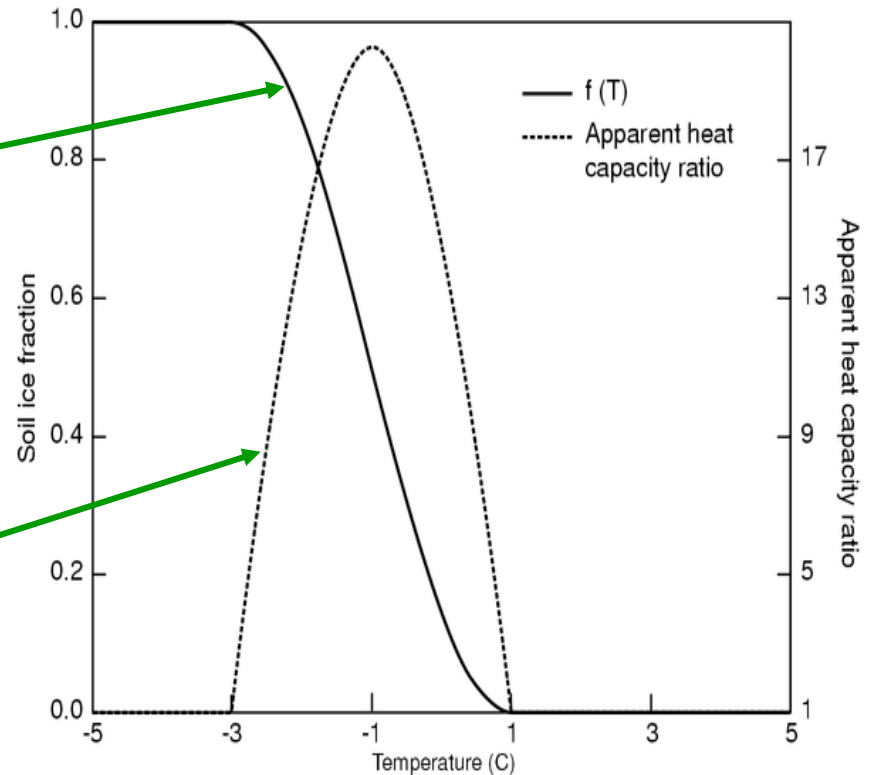
$$(\rho C)_s \frac{\partial T}{\partial t} = \frac{\partial}{\partial z} \lambda_T \frac{\partial T}{\partial z} + L_f \rho_w \frac{\partial \theta_I}{\partial t}$$

θ_I Soil frozen water

$$\theta_I = \theta_I(T) = f(T) \theta$$

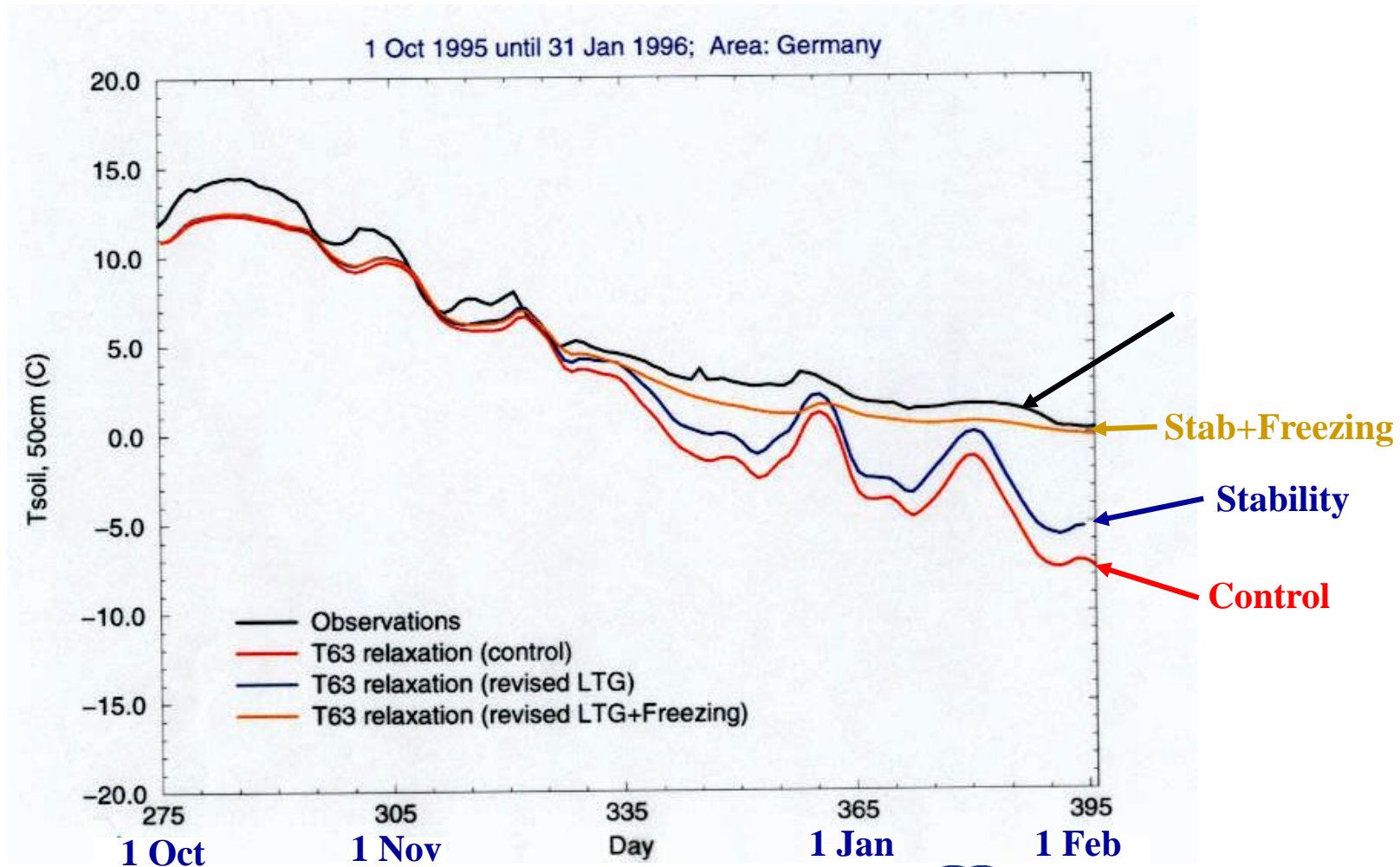
$$\left[(\rho C)_s - L_f \rho_w \theta \frac{\partial f}{\partial T} \right] \frac{\partial T}{\partial t} = \frac{\partial}{\partial z} \lambda_T \frac{\partial T}{\partial z}$$

Apparent heat capacity



Case study: winter (4)

Germany soil temperature: Observations vs Long model relaxation integrations



Recap: The surface energy equation

$$(1 - \alpha)R_S^\downarrow + \varepsilon_g R_T^\downarrow - \varepsilon_g \sigma T_{sk}^4 + \rho C_h u_L (C_p T_L + gz - C_p T_{sk}) + \rho C_h u_L [a_L q_L - a_s q_{sat}(T_{sk}, p_s)] + G(T_s, T_{sk}) = (\rho C)_g D \frac{\partial T_s}{\partial t}$$

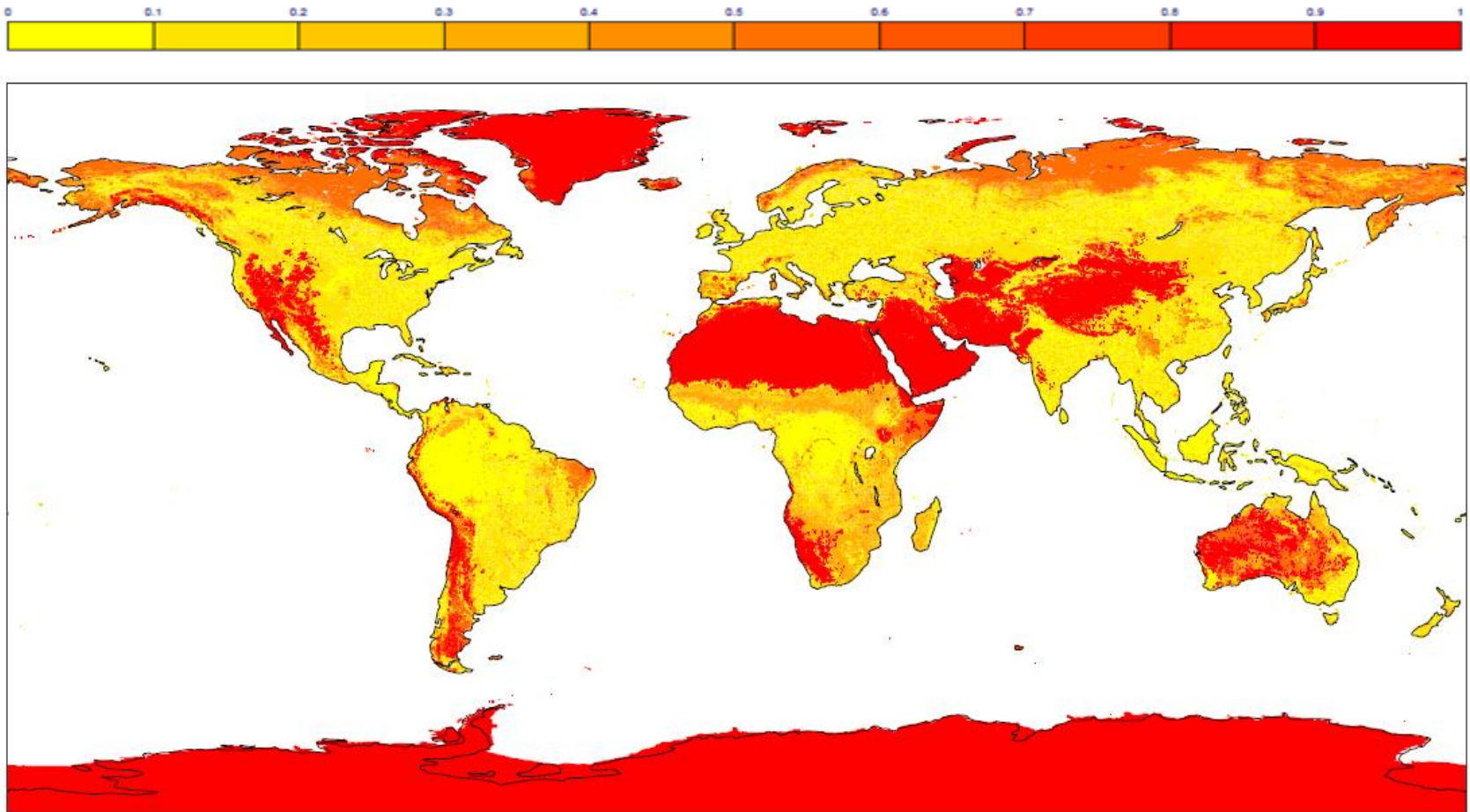
● Equation for T_s, T_{sk}

● For:

- a thin soil layer at the top $(\rho C)_g D \frac{\partial T_s}{\partial t} \approx 0$
- $G(T_s, T_{sk})$ is known, or parameterized or $G \ll R_n$

we have a non-linear equation defining the skin temperature

Bare ground fraction



Calculated from GLCC 1km
and assigned vegetation covers

Bare ground evaporation

- Soil (**bare ground**) evaporation is due to:
 - Molecular diffusion from the **water in the pores of the soil matrix** up to the interface soil atmosphere (z_{0q})
 - Laminar and turbulent diffusion in the air between z_{0q} and screen level height
- All methods are sensitive to the **water in the first few cm of the soil** (where the water vapour gradient is large). In very dry conditions, water vapour inside the soil becomes dominant

α method

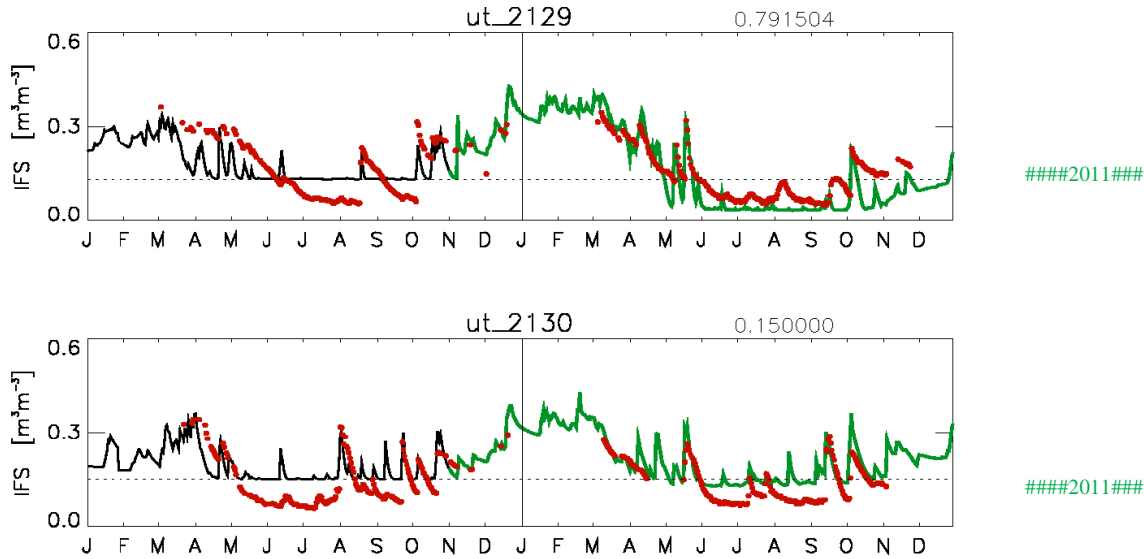
$$E = \rho \frac{q_L - \alpha q_{sat}(T_{sk})}{r_a}$$

$\alpha = f(\theta_1)$ "Relative humidity of the soil"

θ_1 Top soil layer (a few cm) water

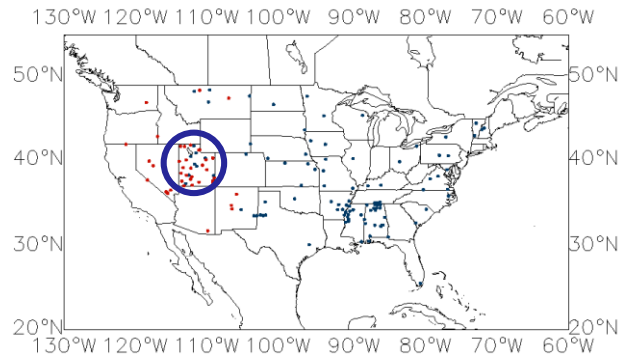
HTESSEL bare soil evaporation

(Balsamo et al. 2011, Albergel et al. 2012)



The introduction of bare ground evaporation revision (green-line) is quite effective in reducing the soil moisture below the wilting point in non-vegetated area (upper panel of figure above, at 79% bare ground, SCAN site in Utah).

$$R_c = R_{\text{soil}} f_2(w_1)$$

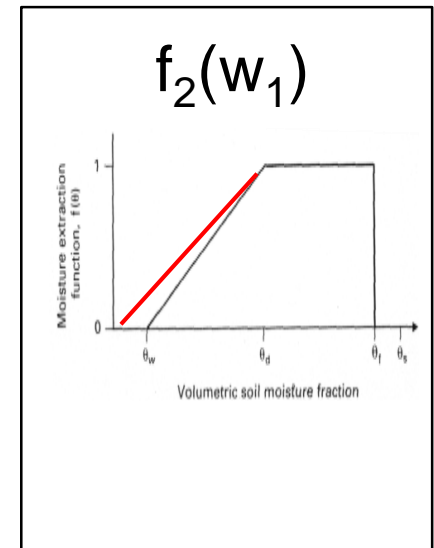


● SOIL Evaporation

alsamo et al. (2011)

based on

Mahfouf and Noilhan (1991)



HTESEL Transpiration

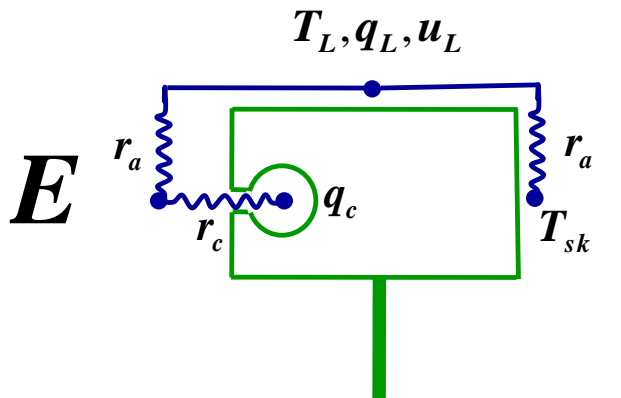
- **Sensible heat (H)**, the resistance formulation

$$H = \rho C_p C_h u_L (T_L - T_{sk}) = \rho C_p \frac{T_L - T_{sk}}{r_a}$$

r_a aerodynamic resistance, $[r_a] = sm^{-1}$

$$r_a = \frac{1}{C_h u_L}$$

- **Evaporation (E)**, the resistance formulation (the **big leaf approximation**, Deardorff 1978, Monteith 1965)

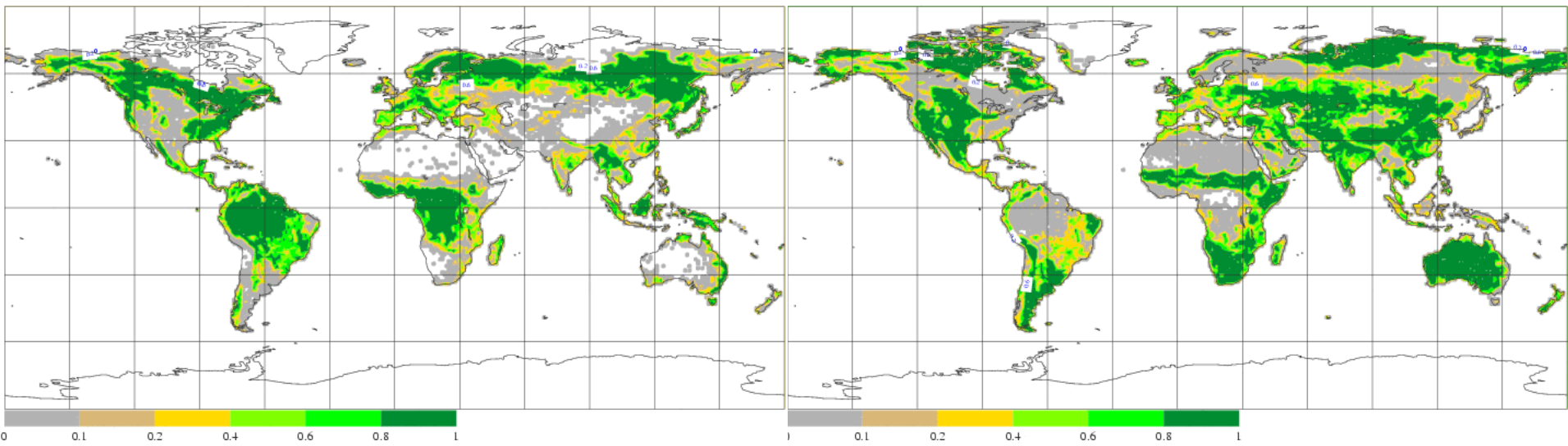


$$E = \rho \frac{q_L - q_c}{r_a + r_c} = \rho \frac{q_L - q_{sat}(T_{sk})}{r_a + r_c}$$

$q_c = q_{sat}(T_{sk})$ Specific humidity for the interior of the stomata, ie, for saturated conditions

r_c canopy resistance

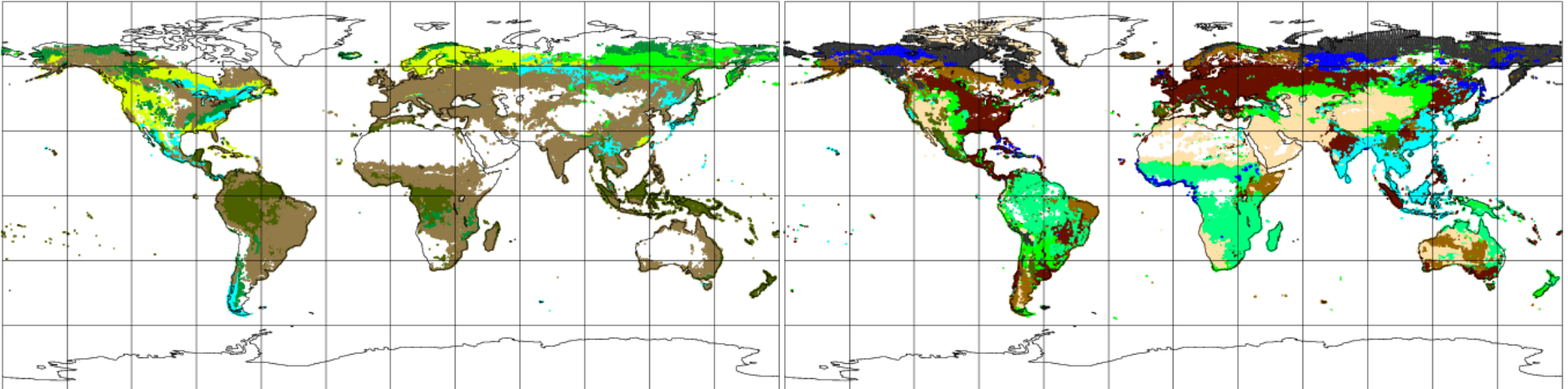
High and Low vegetation fractions



Aggregated from GLCC 1km

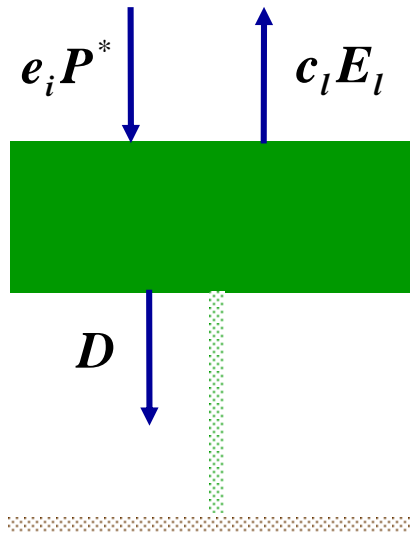
High and Low vegetation types

■ ever needle ■ deci needle ■ deci broad ■ ever broad ■ mix forest ■ int forest ■ crops ■ sh grass ■ ta grass ■ tundra ■ irr crops ■ semidesert ■ bog/marsh ■ ever shrub ■ deci shrub



Aggregated from GLCC 1km

Interception: Canopy water budget



$$\frac{\partial w_l}{\partial t} = e_i P^* + c_l E_l + D = I + c_l E_l$$

w_l Intercepted water

e_i efficiency of interception

P^* modified precipitation

$c_l E_l$ evaporation of intercepted water

D rate of drainage at the bottom of the canopy

HTESSSEL: interception

- Interception layer for rainfall and dew deposition

$$\frac{\partial w_l}{\partial t} = I + c_l E_l$$

$$I = \max\left(e_i c_l P^*, \frac{w_{lmax} - w_l^n}{\Delta t}\right)$$

$P^* = P / k$ **modified precipitation**

k **fraction of grid - box covered by precipitation**

$T = P - I$ **Throughfall (input to top soil)**

Soil science miscellany

- The soil is a 3-phase system, consisting of
 - minerals and organic matter **soil matrix**
 - water **condensate (liquid/solid) phase**
 - moist air trapped **gaseous phase**
- **Texture** - the size distribution of soil particles

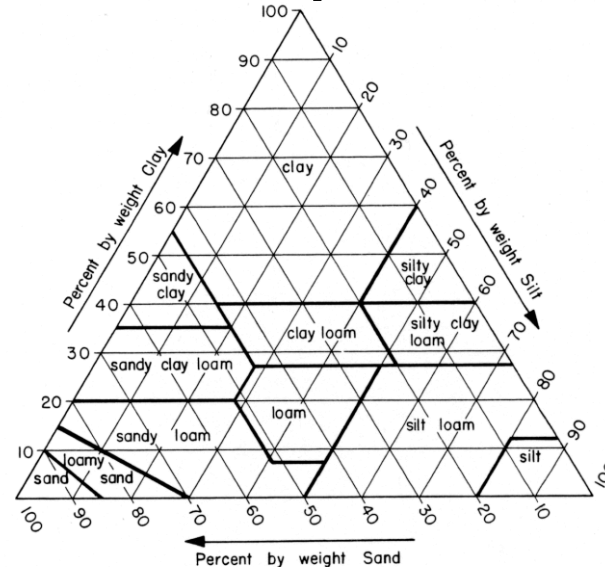
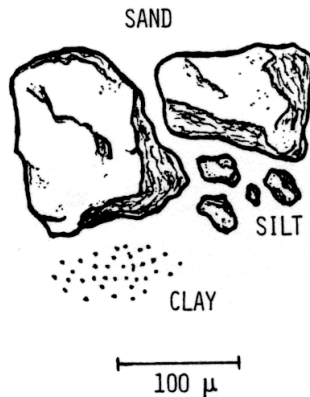


Fig. 3.5. Textural triangle, showing the percentages of clay (below 0.002 mm), silt (0.002–0.05 mm), and sand (0.05–2.0 mm) in the basic soil textural classes.

Soil properties

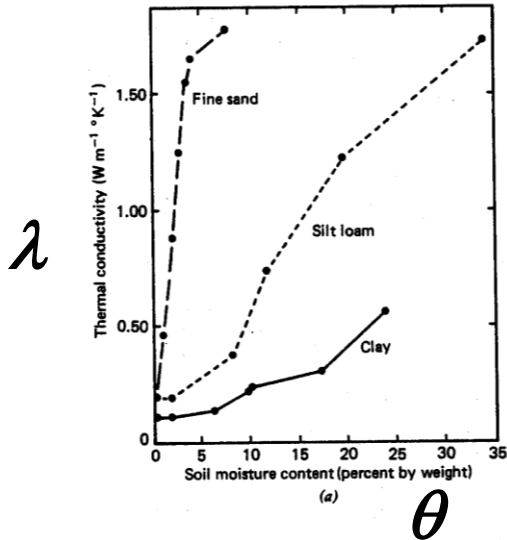


Table 4.1
Molecular Thermal Properties of Natural Materials^a

Material	Condition	Mass density ρ ($\text{kg m}^{-3} \times 10^3$)	Specific heat c ($\text{J kg}^{-1} \text{K}^{-1} \times 10^3$)	Heat capacity C ($\text{J m}^{-3} \text{K}^{-1} \times 10^6$)	Thermal conductivity k ($\text{W m}^{-1} \text{K}^{-1}$)	Thermal diffusivity α_h ($\text{m}^2 \text{sec}^{-1} \times 10^{-6}$)
Air	20°C, Still	0.0012	1.00	0.0012	0.026	21.5
Water	20°C, Still	1.00	4.19	4.19	0.58	0.14
Ice	0°C, Pure	0.92	2.10	1.93	2.24	1.16
Snow	Fresh	0.10	2.09	0.21	0.08	0.38
Sandy soil	Dry	1.60	0.80	1.28	0.30	0.24
(40% pore space)	Saturated	2.00	1.48	2.98	2.20	0.74
Clay soil	Dry	1.60	0.89	1.42	0.25	0.18
(40% pore space)	Saturated	2.00	1.55	3.10	1.58	0.51
Peat soil	Dry	0.30	1.92	0.58	0.06	0.10
(80% pore space)	Saturated	1.10	3.65	4.02	0.50	0.12

^a After Oke (1987).

More soil science miscellany

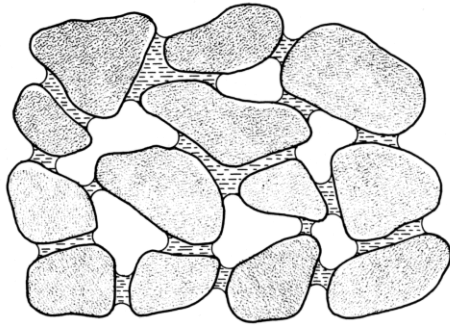


Fig. 7.1. Water in an unsaturated coarse-textured soil.

TABLE I

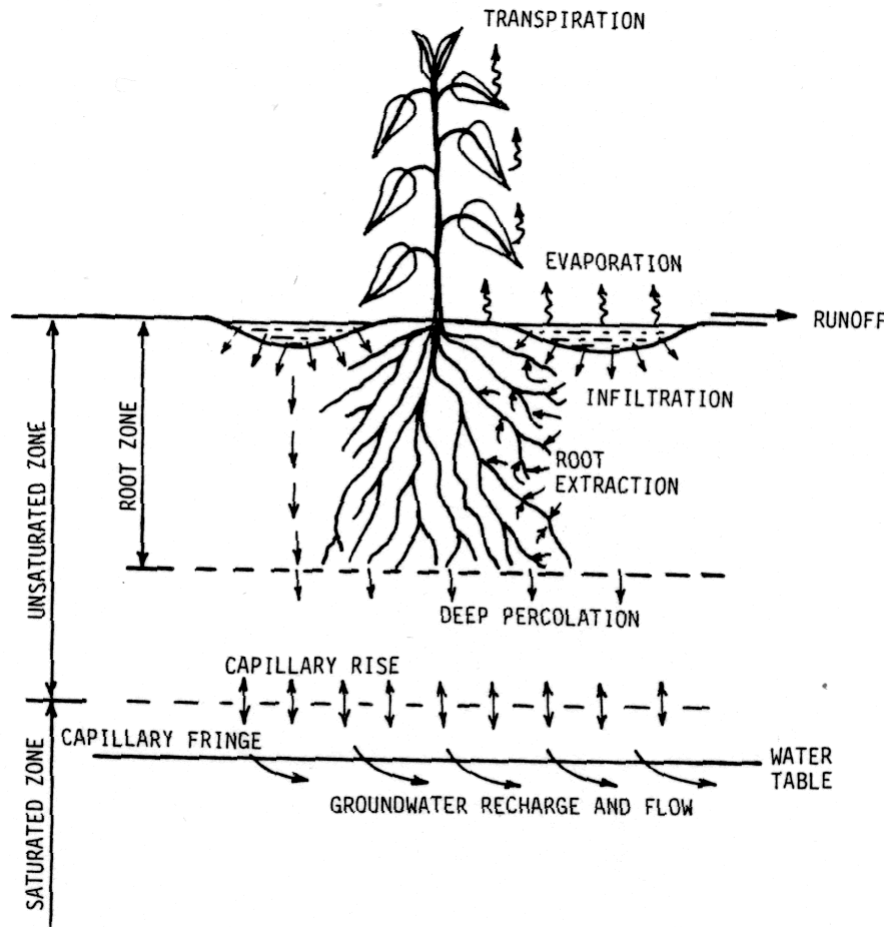
Critical water contents of soils derived from the classification of Clapp and Hornberger (1978): saturated moisture w_{sat} , field capacity w_{fc} , wilting point w_{wilt} . The field capacity is associated with a hydric conductivity of 0.1 mm/day. The wilting point corresponds to a moisture potential of -15 bar

Soil type	w_{sat} (m^3/m^3)	w_{fc} (m^3/m^3)	w_{wilt} (m^3/m^3)
Sand	0.395	0.135	0.068
Loamy sand	0.410	0.150	0.075
Sandy loam	0.435	0.195	0.114
Silt loam	0.485	0.255	0.179
Loam	0.451	0.240	0.155
Sandy clay loam	0.420	0.255	0.175
Silty clay loam	0.477	0.322	0.218
Clay loam	0.476	0.325	0.250
Sandy clay	0.426	0.310	0.219
Silty clay	0.482	0.370	0.283
Clay	0.482	0.367	0.286

● 3 numbers defining soil water properties

- **Saturation (soil porosity)** Maximum amount of water that the soil can hold when all pores are filled **$0.472 \text{ m}^3\text{m}^{-3}$**
- **Field capacity** “Maximum amount of water an entire column of soil can hold against gravity” **$0.323 \text{ m}^3\text{m}^{-3}$**
- **Permanent wilting point** Limiting value below which the plant system cannot extract any water **$0.171 \text{ m}^3\text{m}^{-3}$**

Schematics



$$\rho_w \frac{\partial \theta}{\partial t} = -\frac{\partial F}{\partial z} + \rho_w S_\theta$$

θ soil water [] = $m^3 m^{-3}$

F Soil water flux [] = $kg m^{-2} s^{-1}$

S_θ Soil water source/sink, ie root extraction

:

Top

Bottom

Root extraction

Fig. 17.1. The water balance of a root zone (schematic).

Soil water flux

$$F = -\rho_w \left(\lambda \frac{\partial \theta}{\partial z} - \gamma \right)$$

λ hydraulic diffusivity $[\lambda] = m^2 s^{-1}$

γ hydraulic conductivity $[\gamma] = m s^{-1}$

Darcy's law

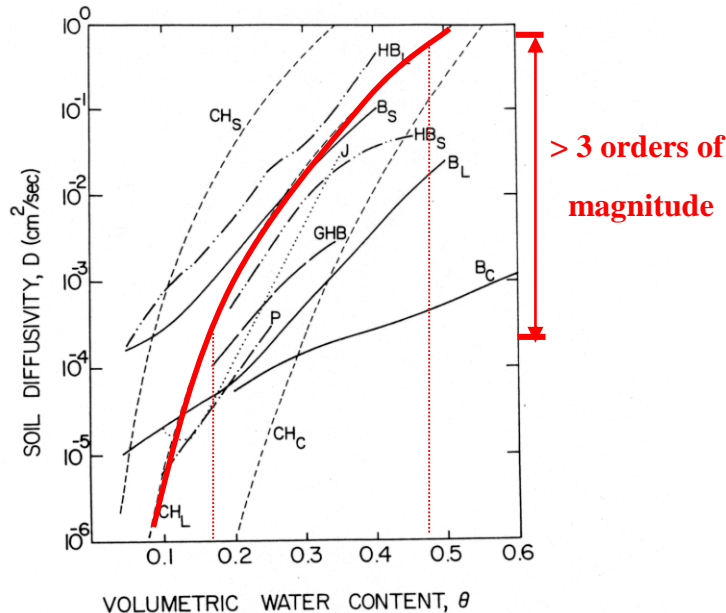


Fig. 2. Examples of the dependence of soil hydraulic diffusivity on volumetric soil water content for loam (HB_L , Hanks and Bowers, 1962); (J, Jackson, 1973); (GHB, Gardner *et al.*, 1970); silt loam (HB_S , Hanks and Bowers, 1962); clay (P, Passioura and Cowan, 1968); results approximated from Gardner (1960) for sand (B_S), loam (B_L), and clay (B_C); relationship from Clapp and Hornberger (1978) for sand (CH_S), loam (CH_L), and clay (CH_C).

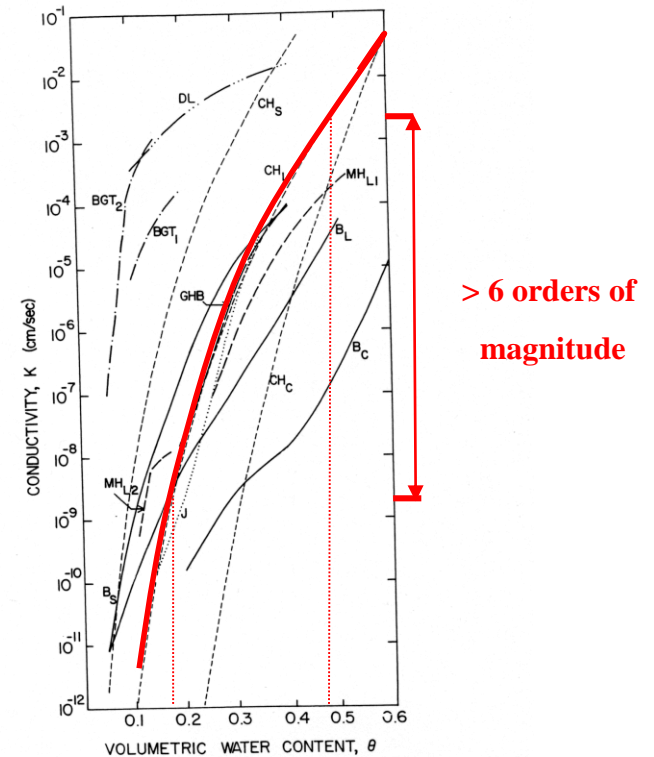


Fig. 3. Examples of the dependence of hydraulic conductivity on volumetric soil water content for sand (DL , Day and Luthin, 1956); (Black *et al.*, 1970, 0–50 cm-BGT₁, 50–150 cm-BGT₂); loam (J, Jackson, 1973); (MH_{L1} and MH_{L2} , Marshall and Holmes, 1979); (GHB, Gardner *et al.*, 1970); results approximated from Gardner (1960) for sand (B_S), loam (B_L), and clay (B_C); relationship from Clapp and Hornberger (1978) for sand (CH_S), loam (CH_L), and clay (CH_C).

HTESSSEL hydrology scheme

- A spatially variable hydrology scheme is being tested following Van den Hurk and Viterbo 2003
- Use of a the Digital Soil Map of World (DSMW) 2003
- Infiltration based on Van Genuchten 1980 and Surface runoff generation based on Dümenil and Todini 1992

$$w(h) = w_r + \frac{w_{sat} - w_r}{(1 + \alpha h)^{1-1/n}} \quad K(h) = K_{sat} \frac{[(1 + \alpha h^n)^{1-1/n} - \alpha h^{n-1}]^2}{(1 + \alpha h^n)^{(1-1/n)(\lambda+2)}} \quad S = 1 - \left(1 - \frac{W}{W_{sat}}\right)^b$$

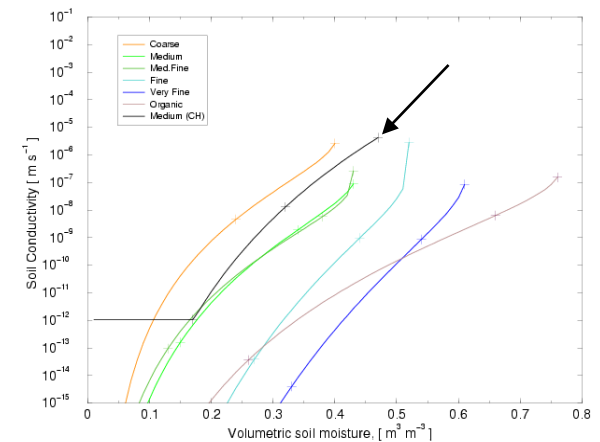
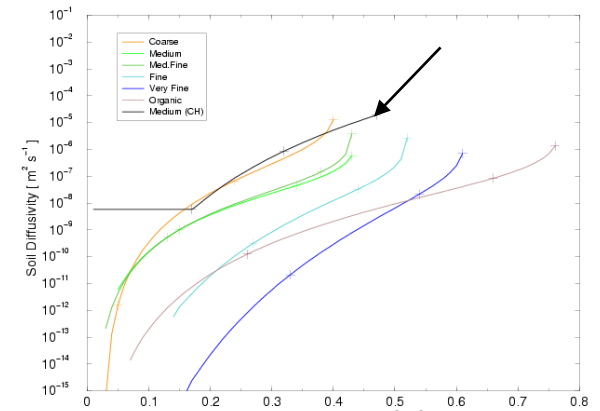
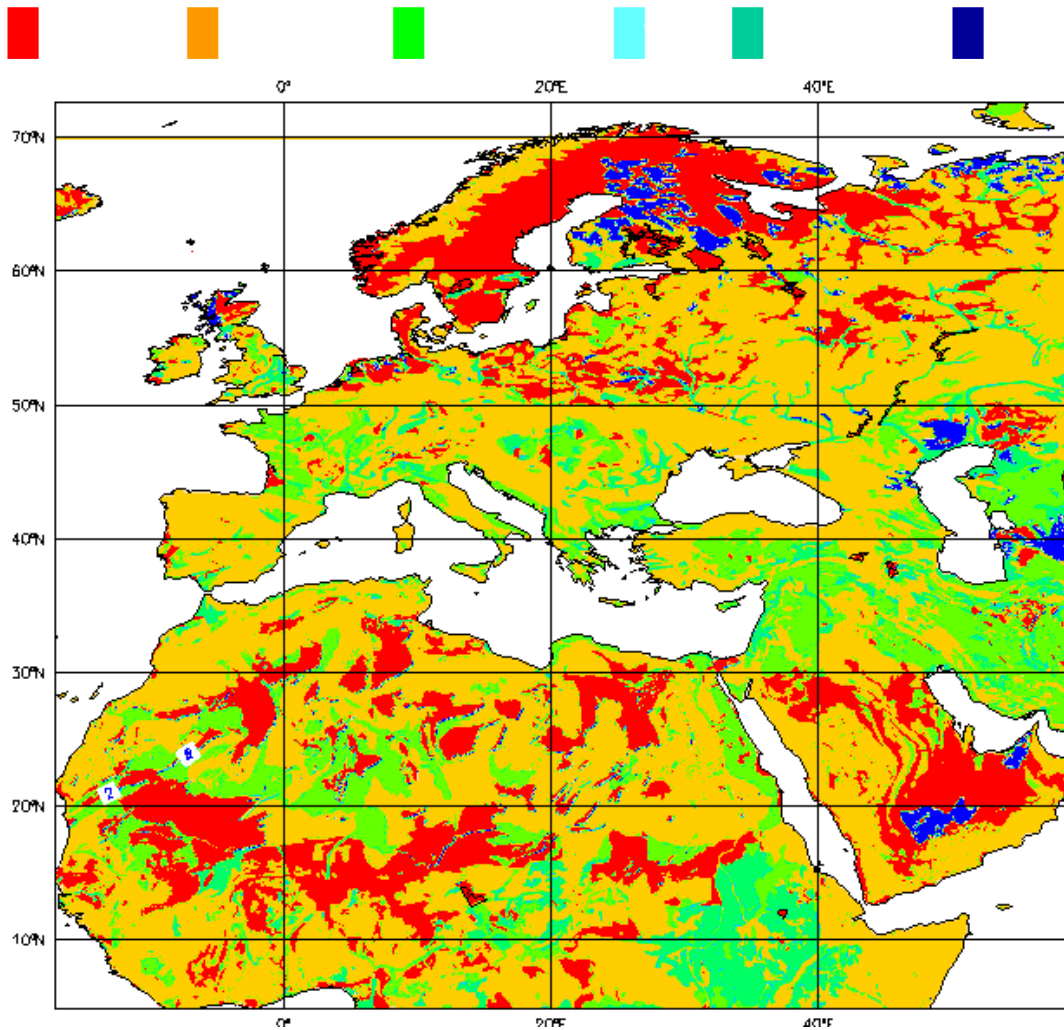
Table 1: Soil type specific Van Genuchten coefficients

Parameter	Symbol	units	Texture class				
			Coarse	Medium	Medium -fine	Fine	Very fine
Saturation soil moisture content	w_{sat}	m^3/m^3	0.403	0.439	0.430	0.520	0.614
Residual soil moisture content	w_r	m^3/m^3	0.025	0.010	0.010	0.010	0.010
Fit parameter	α	m^{-1}	3.83	3.14	0.83	3.67	2.65
Fit parameter	λ	-	1.250	-2.342	-0.588	-1.977	2.500
Fit parameter	n	-	1.38	1.18	1.25	1.10	1.10
Saturated hydraulic conductivity	K_{sat}	$10^{-6} m/s$	6.94	1.16	0.26	2.87	1.74

$$b = 0.01 \leq \frac{\sigma_o - \sigma_{min}}{\sigma_o + \sigma_{max}} \leq 0.5$$

$$R_s = T - (W_{sat} - W) + W_{sat} \left[\left(1 - \frac{W}{W_{sat}}\right)^{1/(b+1)} - \left(\frac{T}{(b+1)W_{sat}}\right) \right]^{b+1}$$

HTESSSEL hydrology scheme(2)



HTESSSEL soil water equations

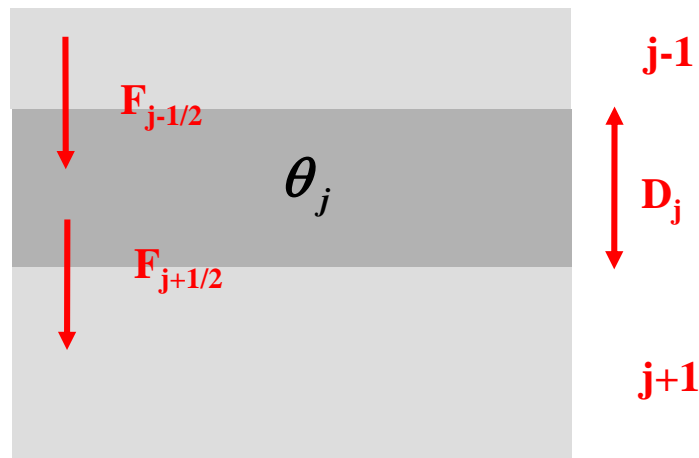
$$\rho_w \frac{(\theta_j^{n+1} - \theta_j^n)}{\Delta t} = - \frac{(F_{j+1/2}^{n+1} - F_{j-1/2}^{n+1})}{D_j} + \rho_w S_{\theta,j}$$

$$F_{j+1/2}^{n+1} = -\rho_w \left(\lambda_{j+1/2} \frac{\theta_{j+1}^{n+1} - \theta_j^{n+1}}{0.5(D_j + D_{j+1})} - \gamma_{j+1/2} \right)$$

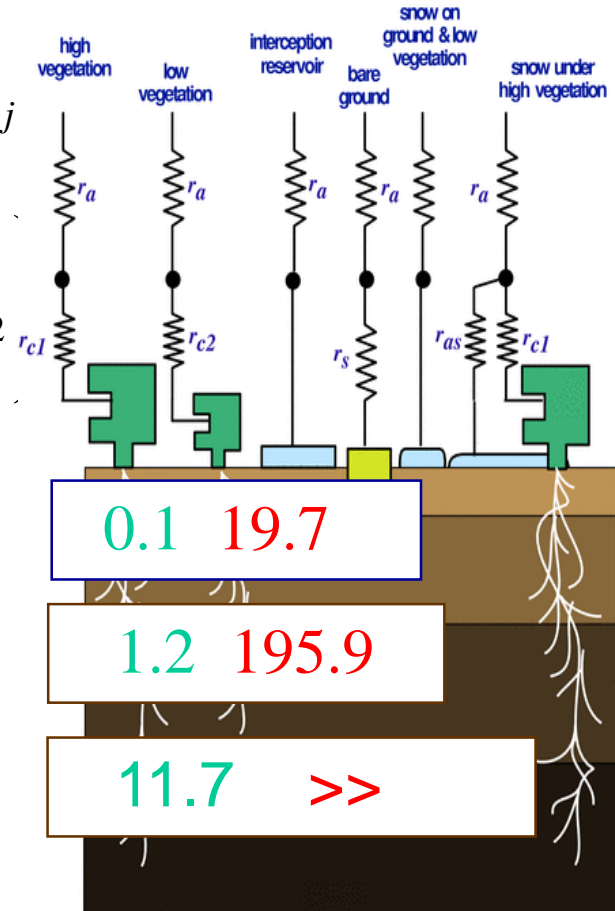
Boundary conditions

$$F_{1/2} = T - Y_s + E_{1/2}$$

$$F_{41/2} = \rho_w \gamma_{41/2}$$



Land surface tiles in ERA40 surface scheme



wet dry

Modelling inland water bodies

A representation of **inland water bodies and coastal areas** in NWP models is essential to simulate large contrasts of albedo, roughness and heat storage

A lake and shallow coastal waters parametrization scheme has been introduced in the ECMWF Integrated Forecasting System combining

HTESSEL

H - Tiled ECMWF

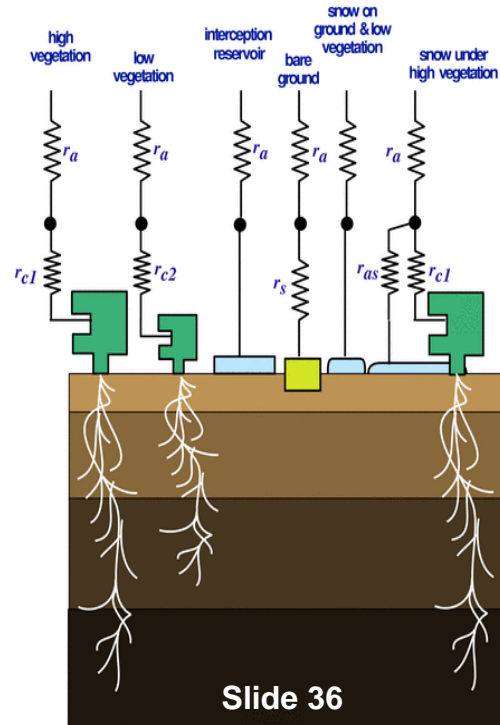
Scheme for Surface Exchanges over Land

+

FLake

Fresh water Lake scheme

Land surface tiles in ERA40 surface scheme



Slide 36

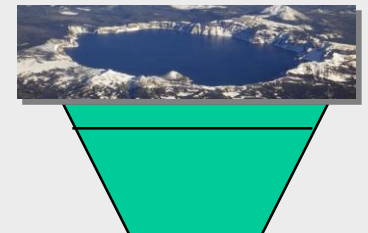
Lake tile

Mironov et al (2010),

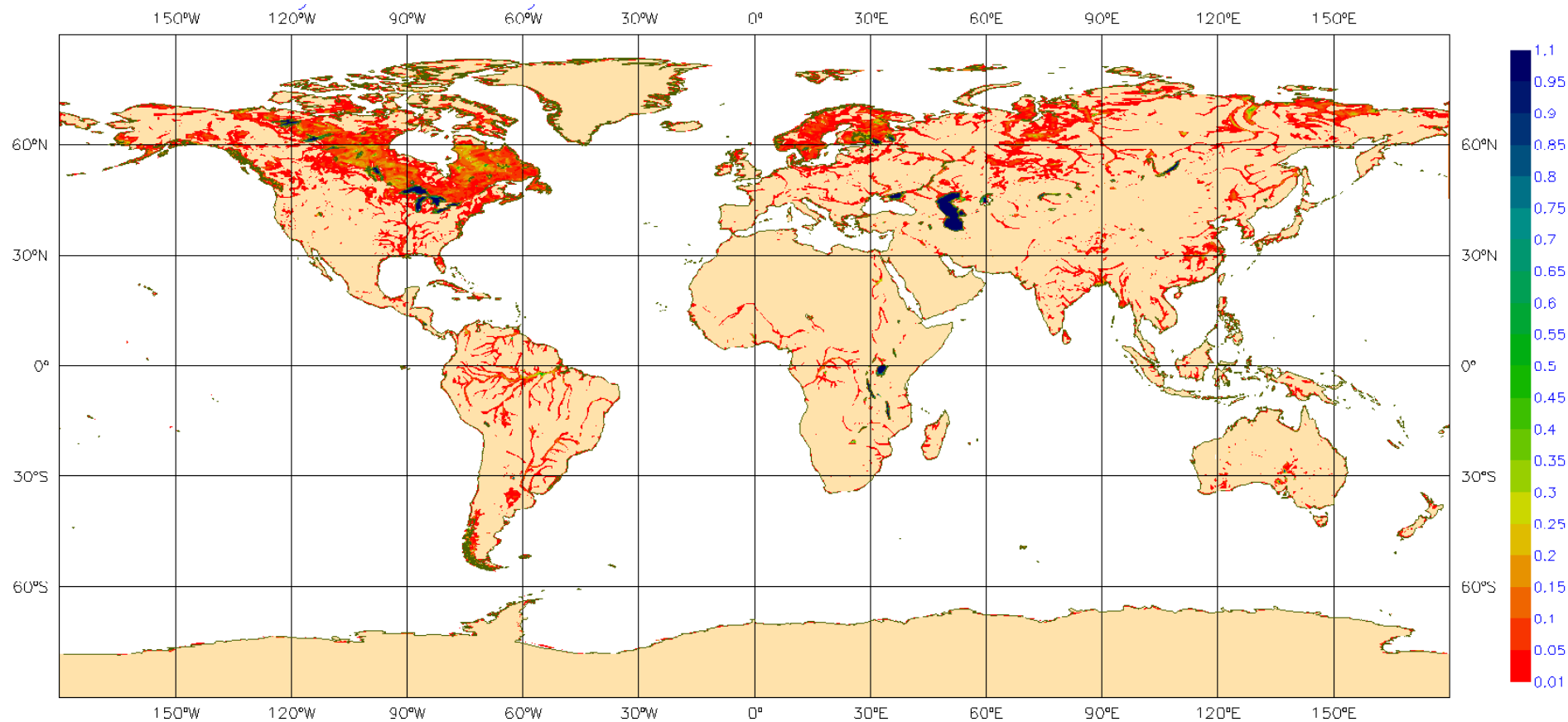
Dutra et al. (2010),

Balsamo et al. (2010, 2012, 2013)

Extra tile (9) to account for sub-grid lakes



Inland water bodies fraction



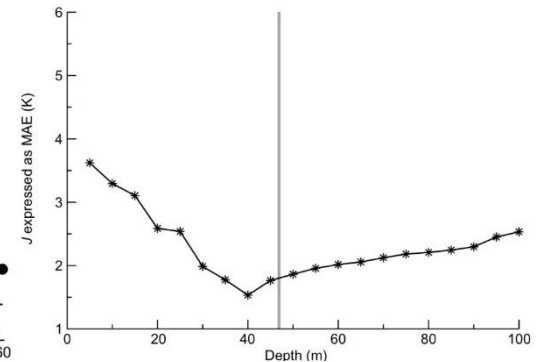
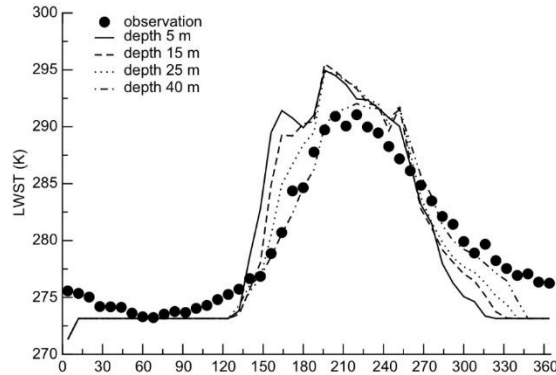
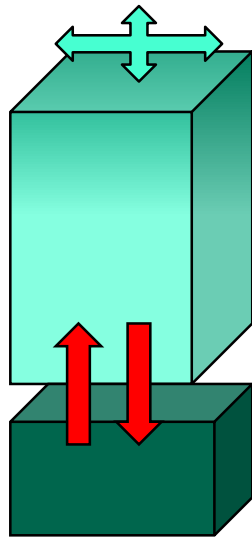
Aggregated from GLOBCOVER 300m

Water bodies heat storage

- All inland water bodies are important energy storage drastically changing sensible heat flux
- FLake (Mironov et al. 2010, BER) <http://lakemodel.net> a two-layer bulk model based on a **self-similar** parametric representation of the evolving temperature profile within lake water and ice
- Introduced in the IFS by Dutra et al. (2010, BER), Balsamo et al. (2010, BER; 2012, TELLUS)



Lake depth is a scalar for lake temperature annual cycle



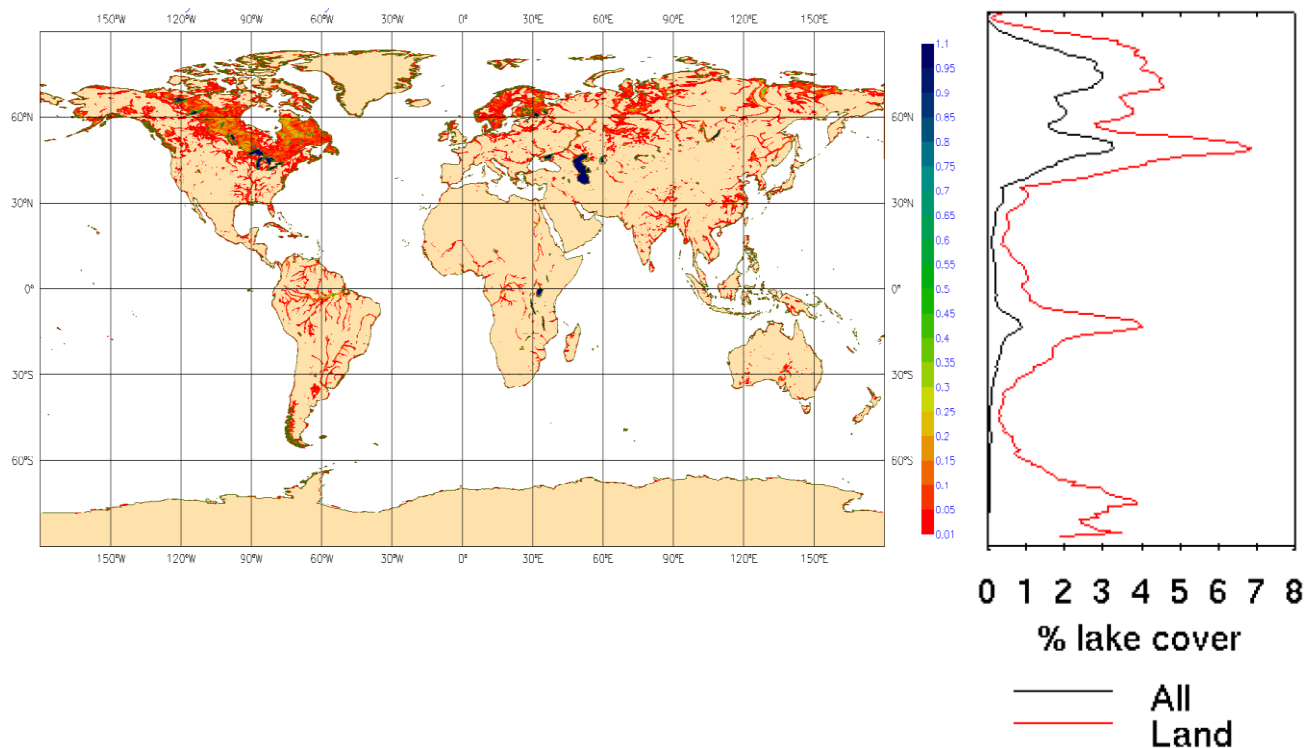
The relationship between the lake temperature (as observed by MODIS) and the lake depth can be used to infer the lake depth in an inversion procedure (Balsamo et al. 2010 BER)

Introduction of Lakes in HTESSEL

Dutra, 2010 (BER), Balsamo et al. 2010 (BER)

A sizeable fraction of land surface has sub-grid lakes: different radiative, thermal roughness characteristics compare to land → affect surface fluxes to the atmosphere

LAKE COVER FRACTION

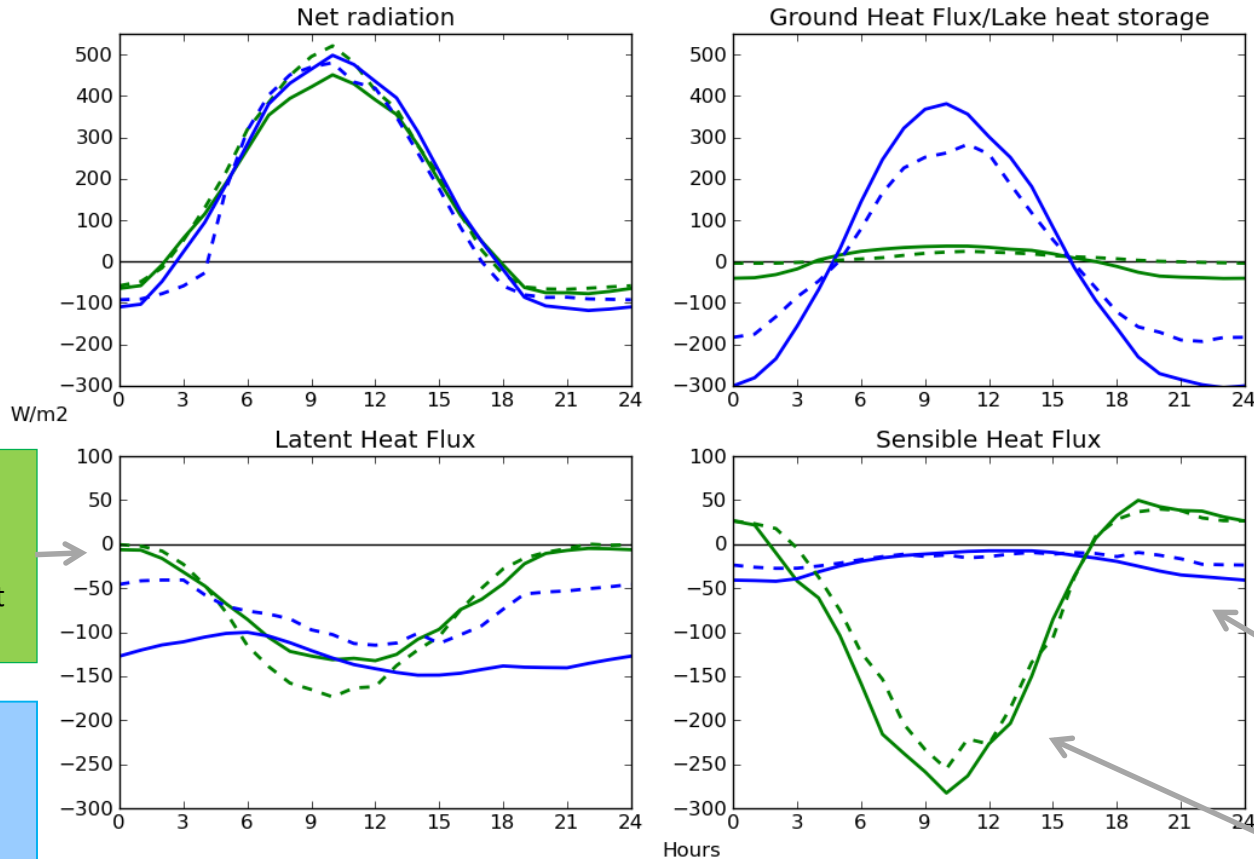


Canada	309/754 41%
USA	175/482 36%
Europe	170/385 44%
Siberia	104/467 22%
Amazon	81/629 13%
Africa	74/584 13%

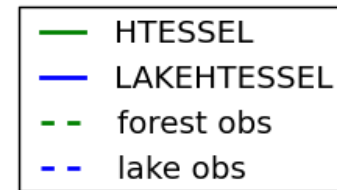
Energy fluxes: Diurnal cycles

Manrique-Suñén et al. (2013, JHM)

Monthly diurnal cycle of energy fluxes for July



Very good representation by the model of diurnal cycles and particularities of each surface



Forest evaporation is driven by vegetation, so it is zero at night

Lake LH diurnal cycle: overestimation in evaporation

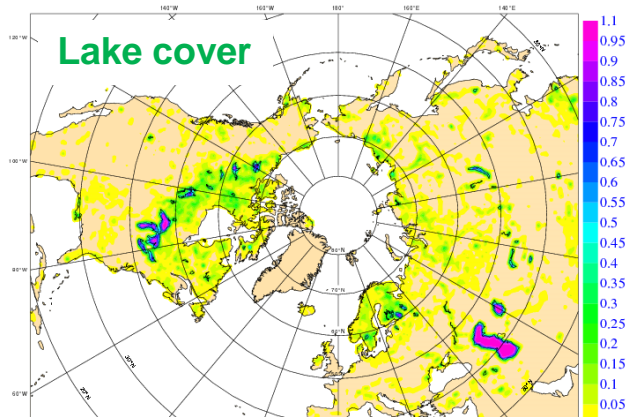
Lake SH maximum is at night

Forest SH maximum is at midday

Main difference between both sites is found in the energy partitioning into SH and G

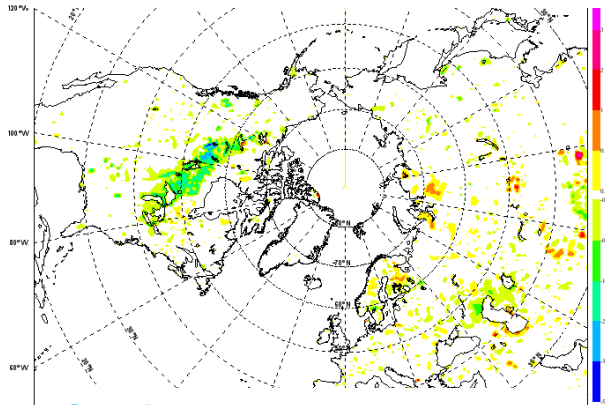
Impact of lakes in NWP forecasts

Balsamo et al. (2012, TELLUS-A) and ECMWF TM 648

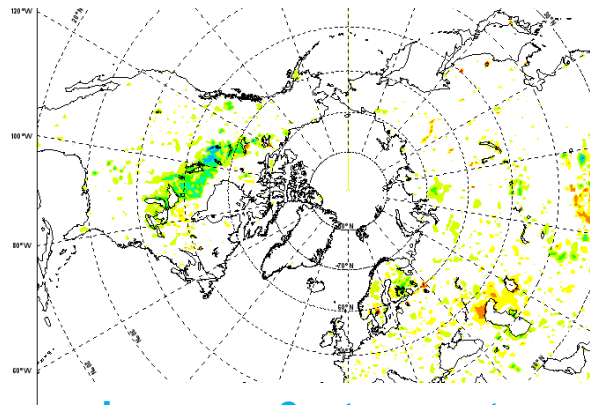


- Forecasts sensitivity and impact of lakes is shown to produce a spring-cooling on lake areas with benefit on the temperatures forecasts (day-2 (48-hour forecast) at 2m.

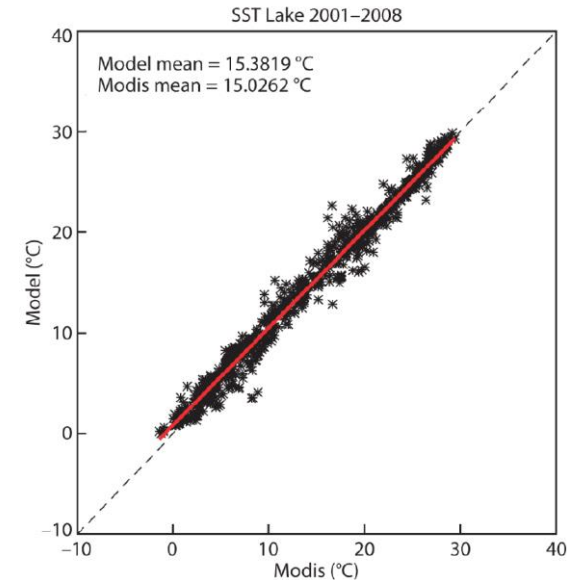
Forecast sensitivity



Cooling 2m temperature
Warming 2m temperature



Improves 2m temperature
Degrades 2m temperature



Lakes are the new added tile to ECMWF land surface scheme that went in operational use on the 12th of May 2015. The importance of lakes and their temperature and ice conditions in generating clouds and storms can be appreciated here:

<http://time.com/9480/great-lakes-frozen-time-lapse-video/>